ELSEVIER

Biophysical Chemistry 59 (1996) 87–94

Biophysical Chemistry

Self-sustained pH oscillations in immobilized proteolytic enzyme systems

Takao Ohmori [1], Ray Y.K. Yang *

Bioreaction Engineering Laboratory, Department of Chemical Engineering, West Virginia University, P.O. Box 6102, Morgantown, WV 26506-6102, USA

Received 15 March 1995; revised 25 September 1995; accepted 2 October 1995

Abstract

This work represents our first step toward fulfilling the need to discover a model system for experimental investigations of temporal oscillations, pattern formations, and other non-linearity related dynamic behavior in immobilized-enzyme–membrane systems. In this paper, the regions in the parameter space where self-sustained pH oscillations can be induced were determined via extensive numerical simulation for five enzyme–membrane systems involving four proteolytic enzymes: α-chymotrypsin, trypsin, bromelain, and ficin. From this study, we concluded that, even with current enzyme-immobilization techniques, the possibility of experimentally observing self-sustained pH oscillations in a flat membrane immobilized with α-chymotrypsin and using *N*-acetyl-L-tryptophan ethyl ester as a substrate is high. Under suitable conditions and with extra efforts, self-sustained oscillations may also occur in membrane systems immobilized with ficin, trypsin and bromelain.

Keywords: Self-sustained oscillations; pH oscillations; Immobilized enzyme; Proteolytic enzyme; Enzyme kinetics; Diffusion

1. Introduction

Many biochemical reaction systems associated with immobilized enzymes are highly non-linear due to the coupling of autocatalytic reactions with diffusion. The non-linearity of such systems, under conditions far from equilibrium, may lead to interesting dynamic behavior, e.g., temporal oscillations, spatial pattern formation, and deterministic chaos [1]. The dynamics of these phenomena is of theoretical as well as practical interests, as their studies may lead to a better understanding of the biological regulations of living cells, and may also contribute to the development of intelligent sensors whose functions are to mimic those of biological systems [2].

There is a strong need for the researchers in the areas of biotechnology and non-linear dynamics to have some simple, robust and easily reproducible immobilized-enzyme systems to serve as model systems for studying the dynamics of non-linear reaction-diffusion systems. However, only a couple of model systems have been reported so far [1,3]; one of them is the immobilized-papain system, which exhibits autonomous pH oscillations as a result of the coupling of a proton-producing, pH-dependent hydrolysis reaction with diffusion. The reaction with its bell-shaped dependence of rate on pH proceeds autocatalytically when the pH is larger than the

* Corresponding author.

[1] On leave from Department of Chemical Systems, National Institute of Materials and Chemical Research, Tsukuba 305, Japan.

SSDI 0301-4622(95)00124-7

optimal pH of the enzyme. Since the revelation by Caplan et al. [4] of the existence of self-sustained autonomous pH oscillations in the papain system through their numerical simulation of a papain membrane, extensive theoretical investigations on this system have been conducted [5–8]. The existence of three steady states, as a result of its sigmoidal dependence of rate on pH in the autocatalytic region, and their stabilities were used by Hardt et al. [6] and Caplan and Naparstek [8] to explain the occurrence of self-sustained oscillations in the papain system. On the other hand, experimental investigations on the autonomous pH oscillations in the same system have been reported only by Naparstek et al. [9] and Ohmori and Yang [10], and so far no definitive experimental confirmation of the existence of self-sustained oscillations (limit cycle) has been achieved. Ohmori and Yang [10], however, have experimentally observed other types of autonomous pH oscillations. They have also discussed in detail various factors which have prevented them from experimentally observing self-sustained pH oscillations in the immobilized-papain system. While some of the barriers associated with the papain–gel system may be overcome in the future, it is obvious that other immobilized-enzyme systems, which are more user-friendly, must be found.

Papain is a proteolytic enzyme which catalyzes the hydrolysis of esters as well as peptide bonds in proteins. A variety of other proteolytic enzymes also catalyze the hydrolysis of esters with a similar mechanism. In the present work, we set out to examine a number of immobilized proteolytic enzyme systems using numerical simulation with experimentally determined kinetic parameters to assess the possibility for self-sustained oscillations to occur in these systems. The ultimate aim of this research is to discover a prototype immobilized-enzyme system which can reliably exhibit self-sustained pH oscillations under experimentally realizable conditions and thus can serve as a model system for future experimental investigations of the dynamic behavior of immobilized-enzyme systems in vitro or in vivo.

In this paper, as a result of extensive computation, we have found that, in addition to the papain–membrane system, self-sustained oscillations can also occur in a membrane system immobilized with α-chymotrypsin, trypsin, bromelain, or ficin. For each system, the region of self-sustained oscillations (ROSSO) in a parameter plane has also been determined, and the possibility of experimentally observing self-sustained oscillations in these systems is discussed.

2. Enzyme systems and reaction kinetics

Shown in Table 1 are the five pairs of enzyme–substrate combination chosen for this investigation, together with the papain–*N*-α-benzoyl-L-arginine ethyl ester (BAEE) system. All of them possess reaction rates that exhibit bell-shaped dependence on pH. Furthermore, experimentally measured kinetic parameters associated with each enzymatic reaction system have also been reported in the literature (see references listed in Table 1) for a sufficiently wide range of pH. Although there are many proteolytic enzymes that can hydrolyze esters, only a very limited number of detailed kinetic studies on such enzymes have been reported. Among the enzymes listed in Table 1, α-chymotrypsin and trypsin are serine proteinases, while bromelain, ficin, and papain are

Table 1
Enzyme systems

No.	Enzyme	Substrate	pH range	$(pH)_{opt}$ [a]	Reference
1	α-chymotrypsin	*N*-acetyl-L-tryptophan ethyl ester (ATEE)	5.04–11.22	8.0	[12,13]
2	trypsin	β-alanylglycine ethyl ester (AGEE)	6.0–10.0	8.2	[14]
3	trypsin	*N*-benzoyl-L-alanine methyl ester (BAME)	6.5–10.0	8.7	[15]
4	bromelain	*N*-α-benzoyl-L-arginine ethyl ester (BAEE)	3.2–9.6	6.4	[16]
5	ficin	*N*-α-benzoyl-L-arginine ethyl ester (BAEE)	4.0–9.5	6.5	[17]
6	papain	*N*-α-benzoyl-L-arginine ethyl ester (BAEE)	3.6–9.56	6.4	[18]

[a] The value of $(pH)_{opt}$ slightly depends on the values of the substrate and the enzyme concentrations.

cysteine proteinases. Although the former are of animal origin while the latter are from plant sources, all of them catalyze the hydrolysis of esters with almost the same mechanism as that associated with papain. Since the structures of the active sites of the enzymes are different, α-chymotrypsin and trypsin have their optimal pH at 8.0–8.7, while the other three are at 6.4–6.5. Table 1 presents the ranges of pH in which the kinetic measurements were conducted, and the results obtained are reported in the references listed in the same row. The rate expressions and their associated kinetic parameters used in this work are only applicable within the corresponding pH ranges. Outside these ranges, any region of self-sustained oscillations (ROSSO) obtained is not considered as experimentally realizable.

The rate expression adopted in the present work [11], with its dependence on the proton concentration, is

$$R = \frac{k_{cat}[E][S]}{K_m C_1 + [S]C_2} \quad (1)$$

where

$$C_1 = 1 + 10^{a}[H^+] + \frac{10^{-b}}{[H^+]} \quad (2)$$

$$C_2 = 1 + 10^{c}[H^+] + \frac{10^{-d}}{[H^+]} \quad (3)$$

and enzyme, substrate, and hydrogen ion concentrations are in mol/m^3.

The functional form of the rate expression given by Eqs. 1–3 is obtained by assuming a two-step reaction mechanism with only one intermediate. Although it is known that a three-step mechanism involving two intermediates may be involved in all the reactions associated with the enzymes shown in Table 1, no sufficient experimental data are available in the literature to determine all the kinetic constants associated with the rate expression related to the three-step mechanism for systems 2–5 listed in Table 1. For system 1, Bender et al. [12] reported all the kinetic constants for the rate expression associated with the three-step reaction mechanism. Their subsequent paper [13] mentioned that their previous data in the alkaline region were in error, but they re-measured and reported only part of the erroneous data. Thus, Eq. 1 was also used for system 1. Suffice it to say here that either a two-step or a three-step reaction mechanism leads to a bell-shaped dependence of rate on pH with a sigmoid branch on the alkaline side, which is the prerequisite for self-sustained oscillations to occur.

The kinetic constants, a, b, c, and d in Eqs. 2 and 3, have been determined via a non-linear least-square method (simplex method) using experimentally obtained data from the literature. The values thus determined for systems 1–5 are presented in Table 2, and are used in the numerical simulation to be described in the next section. Note that the Michaelis constant, K_m, and the intrinsic rate constant, k_{cat}, used for each system are also listed in Table 2.

3. Mathematical model and numerical simulation

The immobilized enzyme membrane system being simulated is illustrated schematically in Fig. 1. The thickness of the membrane, L, is small compared to the other dimensions of the membrane. Only one side of the membrane is exposed to the substrate

Table 2
Kinetic constants

System	Kinetic constants					
	k_{cat} (1/s)	K_m (mol/m^3)	a	b	c	d
1	4.40×10^{1}	1.10×10^{-1}	3.80	– [a]	3.65	6.26
2	2.64	3.42×10^{1}	3.97	6.37	4.11	5.74
3	2.65×10^{-1}	1.06×10^{2}	4.13	7.59	3.65	6.50
4	5.17×10^{-1}	1.89×10^{2}	0.70	6.00	0.90	5.50
5	1.15×10^{1}	4.78×10^{1}	1.60	5.43	2.00	5.27

[a] This means $10^{-b} = 0$.

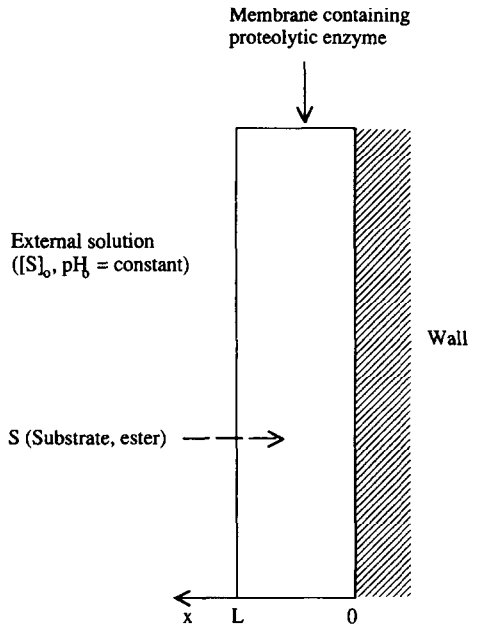

Fig. 1. Immobilized-enzyme–membrane system.

solution in which the concentrations of both substrate and hydrogen ion are kept constant. As the substrate diffuses into the membrane, it is catalytically hydrolyzed by the enzyme contained therein, and hydrogen ion is liberated in the membrane. Because of the bell-shaped dependence of the reaction rate on pH, autocatalysis is induced in the region where pH is larger than pH_{opt}, the optimal pH of the enzyme system. Thus, under appropriate conditions, self-sustained oscillations occur as a result of coupled diffusion and autocatalysis.

The following one-dimensional parabolic partial differential equations are sufficient to simulate the transient variations of pH and substrate concentration of the membrane system [4,11]:

$$\frac{\partial[S]}{\partial t} = -R + D_S \frac{\partial^2[S]}{\partial x^2} \tag{4}$$

$$\frac{\partial A}{\partial t} = R + D_H \frac{\partial^2 A}{\partial x^2} \tag{5}$$

where

$$A = [H^+] - [OH^-] \tag{6}$$

The effective diffusion coefficient of the hydroxyl ion in the membrane is assumed to be the same as that of the hydrogen ion. It is also assumed that the electrical effect can be neglected. The accompanying initial and boundary conditions are:

$$[S] = 0,\ [H^+] = [H^+]_0 \text{ at } t = 0 \text{ for } 0 \le x \le L \tag{7}$$

$$\frac{\partial[S]}{\partial x} = 0,\ \frac{\partial A}{\partial x} = 0 \text{ at } x = 0 \text{ for } t > 0 \tag{8}$$

$$[S] = [S]_0,\ [H^+] = [H^+]_0 \text{ at } x = L \text{ for } t > 0 \tag{9}$$

Introducing the following dimensionless variables: $U = [S]/[S]_0$, $V = A/[S]_0$, $\theta = D_H t/L^2$, $\eta = x/L$, and the dimensionless parameter: $\phi = k_{cat} L^2/D_H$, Eqs. 1, 4, and 5, together with the initial and boundary conditions, Eqs. 7–9, are transformed, respectively, into

$$\frac{\partial U}{\partial \theta} = -R' + \frac{D_S}{D_H} \frac{\partial^2 U}{\partial \eta^2} \tag{10}$$

$$\frac{\partial V}{\partial \theta} = R' + \frac{\partial^2 V}{\partial \eta^2} \tag{11}$$

$$U = 0,\ V = \frac{A_0}{[S]_0} \text{ at } \theta = 0 \text{ for } 0 \le \eta \le 1 \tag{12}$$

$$\frac{\partial U}{\partial \eta} = 0,\ \frac{\partial V}{\partial \eta} = 0 \text{ at } \eta = 0 \text{ for } \theta > 0 \tag{13}$$

$$U = 1,\ V = \frac{A_0}{[S]_0} \text{ at } \eta = 1 \text{ for } \theta > 0 \tag{14}$$

where

$$R' = \frac{\phi[E]U}{K_m C_1 + U[S]_0 C_2} \tag{15}$$

Note that R' is dimensionless, and $\phi^{0.5}$ is the Thiele modulus closely related to the effectiveness factor [19] of this heterogeneous biocatalyst system.

From the above equations, it is clear that four parameters, i.e., $\phi[E]$, D_S/D_H, $[S]_0$ and $[A]_0$ ($[H^+]_0$ or pH_0), alone completely dictate the dynamic behavior of each system. Note that L, membrane thickness, is included in $\phi[E]$ and thus is not an independent parameter. On the other hand, since L and $[E]$ belong to the same group, their values can be varied coordinatively, during an experiment, while keeping the value of $\phi[E]$ unchanged. Though obvious, this point nevertheless has significant experimental im-

plications, and makes the plots generated in this work more useful.

Eqs. 10–15 were solved numerically via a finite difference method using time and space increments which were well below the threshold of numerical instability. Since the substrates listed in Table 1 are of comparable sizes, a value of 0.1 was used for D_S/D_H throughout the simulations [10]. Hence, all the results on ROSSO, to be presented in the next section, are plotted in terms of the three remaining parameters: ϕ[E], $[S]_0$ and pH_0.

4. Results and discussion

While the simulated pH oscillations have been found to occur at any points within the immobilized enzyme membrane, we have focused our investigation only on pH oscillations at $x = 0$ (see Fig. 1). All the ROSSOs reported in this paper refer to oscillations at $x = 0$, as it is the location in the membrane where pH can easily be measured experimentally [10]. This is in line with the purpose of this work, that is to provide a practical guide for rational a priori selection of enzymes for use in future experimental investigations, rather than to conduct an in-depth theoretical analysis of limit cycle in a particular enzyme membrane system.

For each system investigated, the ROSSO corresponding to a given ambient pH, pH_0, is expressed as a closed region in the two-dimensional parameter space of $[S]_0$ vs. ϕ[E]. The rest of the parameter plane represents the region where other types of transient behavior, such as no oscillation and damped oscillations, may take place. Only self-sustained oscillations with an amplitude of more than one pH unit are included in the ROSSO. Hence, the sizes of the ROSSOs shown in this paper are in general on the conservative side.

Fig. 2a and b exhibit, respectively, the bell-shaped dependence of the reaction rate, R, on pH and the ROSSOs corresponding to three different pH_0 values, for the α-chymotrypsin–*N*-acetyl-L-tryptophan ethyl ester (ATEE) system. Note that the values of pH_0 shown in Fig. 2b are all within the pH range where the kinetic measurements were carried out (see Table 1). Furthermore, the values of $[S]_0$ (1.29–2.53 mol/m^3) and ϕ[E] (1.04–6.86 mol/m^3) of the

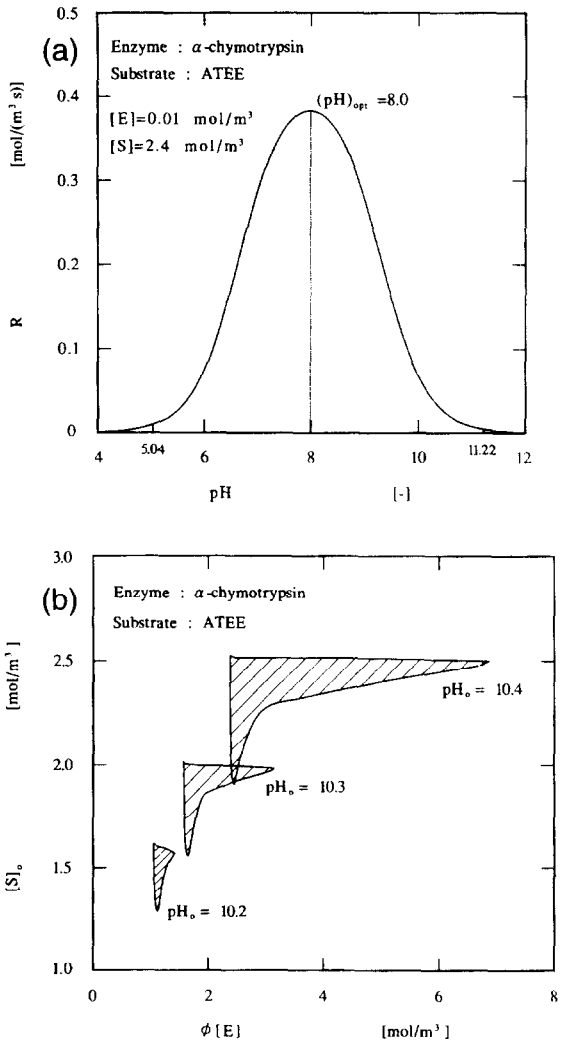

Fig. 2. (a) Bell-shaped dependence of reaction rate on pH (α-chymotrypsin–*N*-acetyl-L-tryptophan ethyl ester). The pH range under which the kinetic measurements reported in [12,13] were conducted is 5.04–11.22. (b) Region of self-sustained oscillations (α-chymotrypsin–*N*-acetyl-L-tryptophan ethyl ester).

ROSSOs are also within experimentally realizable ranges. Hence, it appears that self-sustained autonomous oscillations can be induced in the α-chymotrypsin–ATEE system under experimentally realizable operating conditions using current enzyme immobilization techniques.

The reaction rates and ROSSOs of systems 2 and 3 (Table 1) where trypsin is involved are shown in Figs. 3 and 4, respectively. The substrates involved

are β-alanylglycine ethyl ester (AGEE) and *N*-benzoyl-L-alanine methyl ester (BAME), respectively. For the trypsin–AGEE system (Fig. 3b), the values of pH_0 and $[S]_0$ of the ROSSOs are also in the experimentally realizable region (see Table 1). However, the values of ϕ[E] corresponding to the ROSSO shown are much higher than those in Fig. 2b, implying a very thick membrane and/or an extremely high enzyme concentration, both difficult to achieve with currently available techniques of producing enzyme gels. Hence, major portions of the ROSSOs, especially those in the ranges of large ϕ[E] values, may not be realized experimentally at present. For the trypsin–BAME system, no ROSSO in the experimentally realizable pH range has been obtained, although one corresponding to a pH_0 of 10.6, which is outside the pH range shown in Table 1, is given in

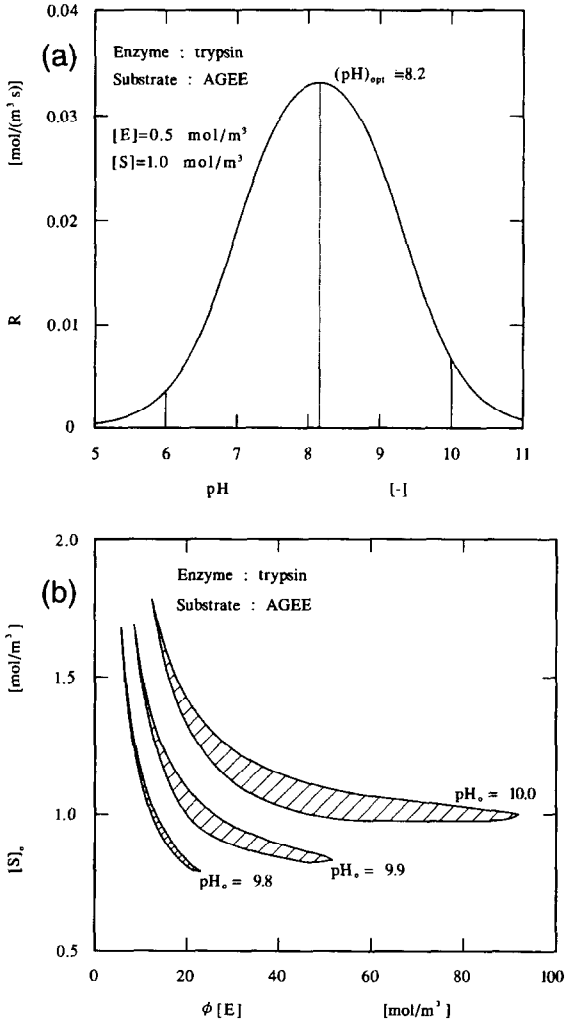

Fig. 3. (a) Bell-shaped dependence of reaction rate on pH (trypsin–β-alanylglycine ethyl ester). The pH range under which the kinetic measurements reported in [14] were conducted is 6.0–10.0. (b) Region of self-sustained oscillations (trypsin–β-alanylglycine ethyl ester).

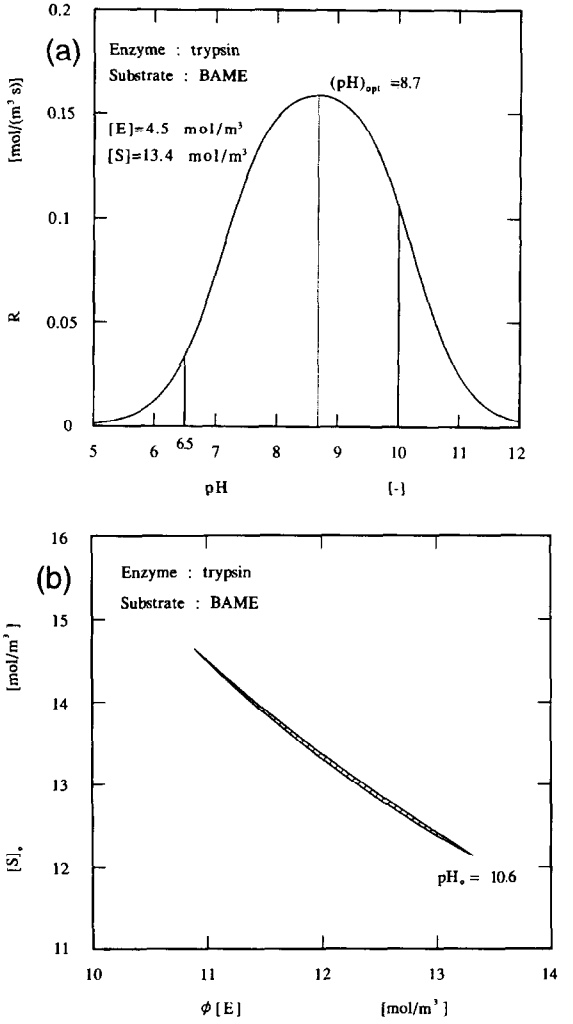

Fig. 4. (a) Bell-shaped dependence of reaction rate on pH (trypsin–*N*-benzoyl-L-alanine methyl ester). The pH range under which the kinetic measurements reported in [15] were conducted is 6.5–10.0. (b) Region of self-sustained oscillations (trypsin–*N*-benzoyl-L-alanine methyl ester).

Fig. 4b for the purpose of comparison with other systems.

Shown in Figs. 5 and 6 are the reaction rates and some typical ROSSOs obtained in each experimentally realizable pH range for the bromelain–BAEE system and the ficin–BAEE system. Except for the upper left tip, the ROSSO for the bromelain–BAEE system is located in the range of ϕ[E] which is almost unrealizable experimentally. As for the ficin–BAEE system, the upper left corners of the

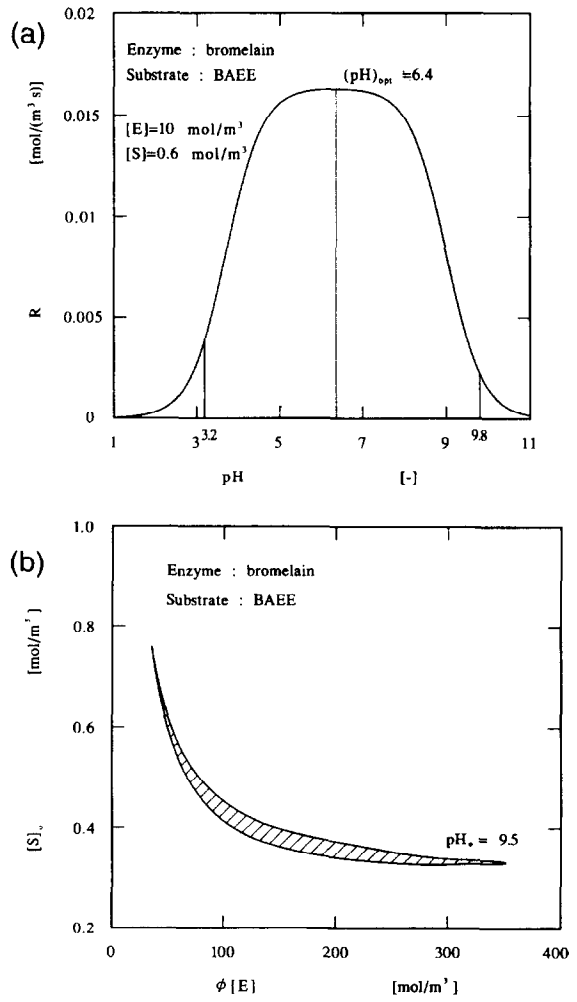

Fig. 5. (a) Bell-shaped dependence of reaction rate on pH (bromelain–*N*-α-benzoyl-L-arginine ethyl ester). The pH range under which the kinetic measurements reported in [16] were conducted is 3.2–9.6. (b) Region of self-sustained oscillations (bromelain–*N*-α-benzoyl-L-arginine ethyl ester).

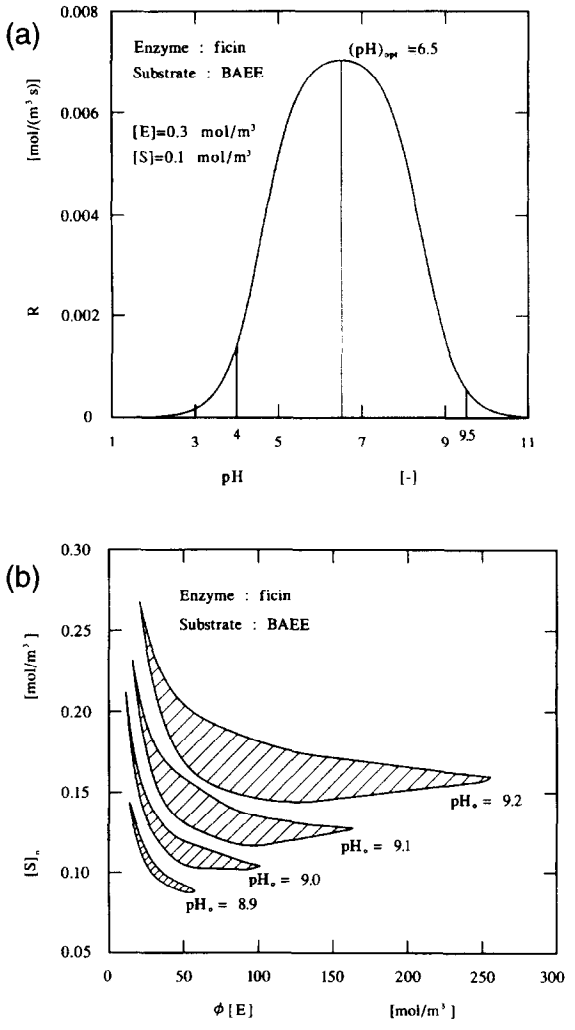

Fig. 6. (a) Bell-shaped dependence of reaction rate on pH (ficin–*N*-α-benzoyl-L-arginine ethyl ester). The pH range under which the kinetic measurements reported in [17] were conducted is 4.0–9.5. (b) Region of self-sustained oscillations (ficin–*N*-α-benzoyl-L-arginine ethyl ester).

ROSSOs are in the experimentally realizable parameters ranges, even though the areas are small.

It is interesting to note that the shapes of ROSSOs for a particular system are similar, and that the typical shape of a ROSSO for the α-chymotrypsin–ATEE system is different from that of other systems. This is obviously a direct reflection of the fact that, for a given enzyme–substrate system, the rate expression with its associated kinetic parameters is

uniquely fixed, while all the other parts of the models are the same. Thus, the rather different ROSSO shape of the α-chymotrypsin–ATEE system is due to the fact that its b value is missing (see Table 1), which leads to a different dependence of R on $[H^+]$ compared to other systems.

5. Conclusions

We have conducted an extensive computational investigation to determine the regions in parameter spaces where self-sustained oscillations in pH can be induced for five immobilized proteolytic enzyme–membrane systems. As a result, we have concluded that self-sustained pH oscillations can occur in all the five systems investigated, although for the four systems involving trypsin, bromelain, and ficin, the self-sustained pH oscillations may occur only in the ranges of parameters which are experimentally difficult to achieve with our current expertise on enzyme immobilization in the membrane. However, the ROSSOs for the α-chymotrypsin–ATEE system are located in the currently experimentally realizable parameters ranges, and hence the possibility of experimentally observing self-sustained pH oscillations in this system is relatively high.

6. Nomenclature

A	$[H^+] - [OH^-]$, as defined in Eq. 6 (mol/m^3)
a,b,c,d	empirically determined kinetic parameters in Eqs. 2 and 3
D	effective diffusion coefficient (m^2/s)
$[E]$	concentration of enzyme (mol/m^3)
$[H^+]$	concentration of hydrogen ion (mol/m^3)
K_m	Michaelis constant (mol/m^3)
k_{cat}	reaction rate constant ($1/s$)
L	thickness of membrane (m)
$[OH^-]$	concentration of hydroxyl ion (mol/m^3)
$(pH)_{opt}$	pH at which reaction rate is maximum
R	reaction rate (mol/m^3 s)
$[S]$	concentration of substrate (mol/m^3)
t	time (s)

Subscripts

H	hydrogen ion
o	external solution
S	substrate

Acknowledgements

We gratefully acknowledge the support of the National Science Foundation, the Wheeling–Nisshin Foundation, the Pittsburgh Supercomputing Center, and the West Virginia NET, and thank James Beach and Diane Hart for their assistance.

References

[1] R. Larter, Chem. Rev., 90 (1990) 355.
[2] K. Yoshikawa and T. Ishii, in M. Kobayashi (Ed.), Physical Organic Chemistry, Elsevier, Amsterdam, 1987, p. 477.
[3] J.F. Hervagault and D. Thomas, Methods Enzymol., 135 (1987) 554.
[4] S.R. Caplan, A. Naparstek and N.J. Zabusky, Nature, 245 (1973) 364.
[5] N.J. Zabusky and R.H. Hardin, Phys. Rev. Lett., 31 (1973) 812.
[6] S. Hardt, A. Naparstek, L.A. Segel and S.R. Caplan, in D. Thomas and J.P. Kernevez (Eds.), Analysis and Control of Immobilized Enzyme Systems, North Holland, Amsterdam, 1976, p. 9.
[7] T.R. Chay, J. Theor. Biol., 80 (1979) 83; Biophys. J., 30 (1980) 99.
[8] S.R. Caplan and A. Naparstek, Adv. Biol. Med. Phys., 16 (1977) 177.
[9] A. Naparstek, D. Thomas and S.R. Caplan, Biochim. Biophys. Acta, 323 (1973) 643.
[10] T. Ohmori and R.Y.K. Yang, Biotechnol. Appl. Biochem., 20 (1994) 67.
[11] K.J. Laidler and P.S. Bunting, The Chemical Kinetics of Enzyme Action, Clarendon Press, Oxford, 2nd edn., 1973.
[12] M.L. Bender, G.E. Clement, F.J. Kézdy and H.d'A. Heck, J. Am. Chem. Soc., 86 (1964) 3680.
[13] M.L. Bender, M.J. Gibian and D.J. Whelan, Proc. Natl. Acad. Sci. USA, 56 (1966) 833.
[14] R. Kobayashi and S. Ishii, J. Biochem., 75 (1974) 825.
[15] H.P. Kassera and K.J. Laidler, Can. J. Chem., 47 (1969) 4021.
[16] T. Inagami and T. Murachi, Biochemistry, 2 (1963) 1439.
[17] J.R. Whitaker, Biochemistry, 8 (1969) 1896.
[18] J.R. Whitaker and M.J. Bender, J. Am. Chem. Soc., 87 (1965) 2728.
[19] J.J. Carberry, Chemical and Catalytic Reaction Engineering, McGraw-Hill, New York, 1976.